

# Multiple mechanisms mediating carbon monoxide inhibition of the voltage-gated K<sup>+</sup> channel Kv1.5

Moza M Al-Owais<sup>1</sup>, Nishani T Hettiarachchi<sup>1</sup>, John P Boyle<sup>1</sup>, Jason L Scragg<sup>1</sup>, Jacobo Elies<sup>1,3</sup>, Mark L Dallas<sup>1,4</sup>, Jon D Lippiat<sup>2</sup>, Derek S Steele<sup>2</sup> and Chris Peers<sup>\*1</sup>

The voltage-gated K<sup>+</sup> channel has key roles in the vasculature and in atrial excitability and contributes to apoptosis in various tissues. In this study, we have explored its regulation by carbon monoxide (CO), a product of the cytoprotective heme oxygenase enzymes, and a recognized toxin. CO inhibited recombinant Kv1.5 expressed in HEK293 cells in a concentration-dependent manner that involved multiple signalling pathways. CO inhibition was partially reversed by superoxide dismutase mimetics and by suppression of mitochondrial reactive oxygen species. CO also elevated intracellular nitric oxide (NO) levels. Prevention of NO formation also partially reversed CO inhibition of Kv1.5, as did inhibition of soluble guanylyl cyclase. CO also elevated intracellular peroxynitrite levels, and a peroxynitrite scavenger markedly attenuated the ability of CO to inhibit Kv1.5. CO caused nitrosylation of Kv1.5, an effect that was also observed in C331A and C346A mutant forms of the channel, which had previously been suggested as nitrosylation sites within Kv1.5. Augmentation of Kv1.5 via exposure to hydrogen peroxide was fully reversed by CO. Native Kv1.5 recorded in HL-1 murine atrial cells was also inhibited by CO. Action potentials recorded in HL-1 cells were increased in amplitude and duration by CO, an effect mimicked and occluded by pharmacological inhibition of Kv1.5. Our data indicate that Kv1.5 is a target for modulation by CO via multiple mechanisms. This regulation has important implications for diverse cellular functions, including excitability, contractility and apoptosis.

*Cell Death and Disease* (2017) 8, e3163; doi:10.1038/cddis.2017.568; published online 2 November 2017

Kv1.5 is a rapidly activating, voltage-gated K<sup>+</sup> channel encoded by *KCNA5* that inactivates slowly and incompletely.<sup>1</sup> Distribution of Kv1.5 is widespread: it is expressed in various cell types in the central nervous system<sup>2,3</sup> and is implicated in certain types of cancers.<sup>4</sup> Kv1.5 is, however, perhaps best studied in the cardiovascular system. Its expression/activity is associated with increased apoptosis in endothelial and smooth muscle cells.<sup>5,6</sup> In vascular smooth muscle cells (VSMCs) of the pulmonary vasculature, it is of particular importance to hypoxic pulmonary vasoconstriction<sup>7–9</sup> and in the development of pulmonary arterial hypertension (PAH).<sup>10–12</sup> Indeed, Kv1.5 expression is reduced in PAH patients<sup>13</sup> and patients with idiopathic PAH possess important single-nucleotide polymorphisms in *KCNA5*, which encodes Kv1.5.<sup>14,15</sup> In the systemic circulation, Kv1.5 also contributes to repolarization of the VSMC membrane potential, limiting Ca<sup>2+</sup> entry and hence vascular tone.<sup>16–18</sup> A recent study employing Kv1.5<sup>-/-</sup> mice has shown that this channel is essential for balancing coronary blood flow with metabolic demands of the working myocardium.<sup>19</sup>

In the heart, Kv1.5 expression is largely confined to the atria where it is responsible for the ultrarapid outward current, I<sub>K<sub>ur</sub>, the major repolarizing current that is active throughout phases 1–3 of the atrial action potential (AP).<sup>20,21</sup> Targeting of Kv1.5 activity/expression is currently regarded as a promising therapeutic approach to the treatment of atrial fibrillation (AF).<sup>22–25</sup></sub>

Given the widespread importance of Kv1.5 in the cardiovascular system and elsewhere, it is perhaps unsurprising that it is regulated via numerous posttranslational modifications, including ubiquitination,<sup>26</sup> sumoylation,<sup>26</sup> palmitoylation,<sup>27</sup> phosphorylation<sup>28,29</sup> and nitrosylation.<sup>30</sup> An additional means of regulation is via its sensitivity to reactive oxygen species (ROS). For example, tonic ROS production by mitochondria or NADPH oxidase (Nox 4) sustains Kv1.5 activity and keeps pulmonary VSMCs relatively hyperpolarized.<sup>31,32</sup> In the coronary circulation, hydrogen peroxide (H<sub>2</sub>O<sub>2</sub>) has been proposed as the signal closely coupling cardiac metabolism to coronary blood flow<sup>33–35</sup> and this coupling appears via H<sub>2</sub>O<sub>2</sub>-mediated augmentation of Kv1.5.<sup>19</sup> Recombinant Kv1.5 activity has also been demonstrated to be directly augmented by H<sub>2</sub>O<sub>2</sub>.<sup>36</sup>

An additional modulator of Kv1.5 is nitric oxide (NO), a long-established, biologically active signalling molecule in the cardiovascular system as well as other tissues.<sup>37–39</sup> NO regulates Kv1.5 via nitrosylation and activation of cGMP,<sup>30</sup> an effect which is of potential importance in the context of AF, given the important role of this channel in atrial electrical activity, and also the fact that NO bioavailability is reduced in AF and NO synthases (NOs) can become uncoupled, leading to superoxide formation.<sup>38,40,41</sup>

Accumulating data continue to establish carbon monoxide (CO) as an important gasotransmitter alongside NO (and hydrogen sulphide), which acts to provide a range of beneficial

<sup>1</sup>Division of Cardiovascular and Diabetes Research, LICAMM, Faculty of Medicine and Health, Faculty of Biological Sciences, University of Leeds, Leeds LS2 9JT, UK and

<sup>2</sup>School of Biomedical Sciences, Faculty of Biological Sciences, University of Leeds, Leeds LS2 9JT, UK

\*Corresponding author: C Peers, Division of Cardiovascular and Diabetes Research, Leeds Institute for Cardiovascular and Metabolic Medicine, Faculty of Medicine and Health, University of Leeds, Clarendon Way, Leeds LS2 9JT, UK. Tel: +44 113 343 4174; Fax: +44 113 343 4803; E-mail: c.s.peers@leeds.ac.uk

<sup>3</sup>Current address: School of Pharmacy and Medical Sciences, University of Bradford, Bradford, UK.

<sup>4</sup>Current address: Reading School of Pharmacy, University of Reading, Reading RG6 6UB, UK.

Received 25.7.17; revised 19.9.17; accepted 21.9.17; Edited by A Finazzi-Agrò

cardiovascular (and other) effects. All three of these gaso-transmitters are products of distinct, widely distributed enzymes.<sup>42,43</sup> CO dilates coronary and other vessels<sup>44–46</sup> and induction of heme oxygenase-1 (HO-1, which produces CO) protects against, for example, myocardial infarction, hypertension and vascular injury.<sup>47,48</sup> CO accounts for many of the effects of HO-1 induction<sup>49–51</sup> and CO inhalation, as well as CO-releasing molecules (CORMs), are being developed for cardiovascular therapy.<sup>52,53</sup> Importantly, HO-1 expression is increased in AF and appears to provide protection against the oxidative stress of this condition.<sup>54–56</sup> Given the important role for Kv1.5 in normal atrial function, its redox sensitivity and the likely involvement of HO-1 as a means of providing protection in AF, we have explored the potential for CO-mediated regulation of Kv1.5 channels using both a recombinant expression system and murine atrial (HL-1) cells.

## Results

**CO inhibits recombinant human Kv1.5.** To examine any potential modulation of Kv1.5 by CO, we applied the CORM, CORM-2, to HEK293 cells stably expressing human Kv1.5 (hKv1.5). As exemplified in the time-series plot of Figure 1a, CORM-2 caused a reversible inhibition of K<sup>+</sup> current amplitudes, and this was associated with a marked slowing of activation kinetics (Figure 1c). By contrast, the inactive form of CORM-2, iCORM, was without significant effect (Figures 1b and c). Inhibition of hKv1.5, and the associated slowing of kinetics, was seen throughout the range of

activation test potentials employed (up to +80 mV; Figure 1d). A concentration–response relationship was constructed using time-series recordings as exemplified in Figure 1a, which yielded an IC<sub>50</sub> value of 23 μM for CORM-2 inhibition of hKv1.5 (Figure 1e).

CO can regulate ion channels via modulation of numerous signalling pathways.<sup>57</sup> To investigate the mechanism of regulation of hKv1.5 by CO, we first explored the involvement of ROS. Figures 2a and b indicate that the ability of CORM-2 to inhibit hKv1.5 was significantly suppressed by a pretreatment of cells (1 h at 37 °C) with either the reducing agent dithiothreitol (DTT, 1 mM) or each of two superoxide dismutase (SOD) mimetics, 5,10,15,20-tetrakis(1-methylpyridinium-4-yl)-21*H*,23*H* porphyrin manganese (III) pentachloride (MnTMPyP; 50 μM), and manganese (III) tetrakis (4-benzoic acid) porphyrin chloride (MnTBAP; 10 μM). All three of these agents significantly, but incompletely, reversed the inhibitory actions of CO, strongly suggesting that ROS contributed to CO-mediated inhibition of hKv1.5. To explore the source of ROS involved in CO-mediated inhibition of Kv1.5, cells were pretreated (1 h at 37 °C) with either diphenylene iodonium (DPI; 3 μM), a non-selective inhibitor of NADPH oxidases, or allopurinol (1 μM), a xanthine oxidase inhibitor. Neither agent altered the ability of CORM-2 to inhibit hKv1.5 (Figures 2c and d). By contrast, pretreatment of cells with mitoTEMPO (10 μM), a mitochondrially targetted antioxidant, almost fully reversed the inhibitory effects of CO (Figures 2c and d). Inhibition of hKv1.5 by CO was also significantly reduced following pretreatment with antimycin A, which inhibits

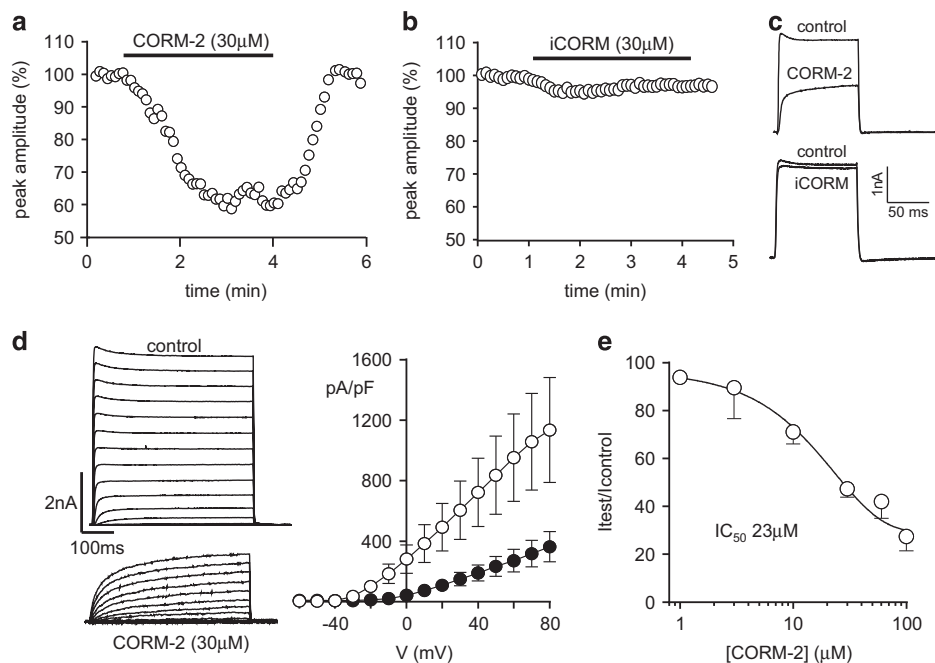


**Figure 1** CO inhibits recombinant hKv1.5. (a) Time-series plot (generated by repeated step depolarizations from – 80 to +50 mV (100 ms duration, 0.2 Hz)) obtained from a HEK293 cell stably expressing human Kv1.5 (hKv1.5). Plot shows normalized peak current amplitudes. For the period indicated by the horizontal bar, the cell was exposed to 30 μM CORM-2. (b) As in panel (a), except this cell was exposed to 30 μM iCORM (inactive breakdown product of CORM-2), as indicated. (c) Example currents from the plotted time series evoked before and during application of CORM-2 (upper) and iCORM (lower). (d) Left, currents evoked in a HEK293 cell expressing hKv1.5 before and during exposure to 30 μM CORM-2, as indicated. Currents were evoked by step-depolarizations from – 60 to +80 mV. Right, Mean (± S.E.M., *n* = 6) current–density versus voltage relationships obtained before (open symbols) and during (solid symbols) application of 30 μM CORM-2. (e) Concentration–response curve for CORM-2 inhibition of hKv1.5. Each point is the mean (± S.E.M., *n* = 3–17 cells in each case) fractional inhibition caused by CORM-2. Data fit yields IC<sub>50</sub> of 23 μM

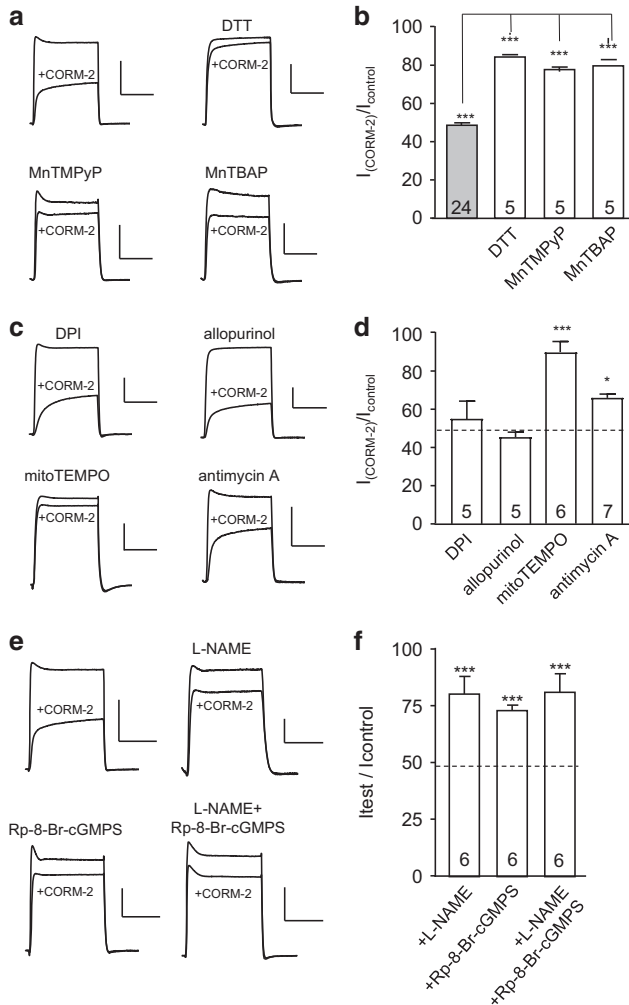


**Figure 2** CO inhibition of hKv1.5 involves mitochondrial reactive oxygen species, NO and soluble guanylyl cyclase. (a) Example currents evoked in hKv1.5-expressing HEK293 cells before and during exposure to 30  $\mu\text{M}$  CORM-2. Currents are examples from time-series studies (as in Figure 1) in which cells were repeatedly depolarized from  $-80$  mV to  $+50$  mV (100 ms duration, 0.2 Hz). CORM-2 was applied either to untreated cells or to cells pretreated for 1 h at  $37^\circ\text{C}$  with DTT (1 mM) MnTMPyP (50  $\mu\text{M}$ ) or MnTBAP (10  $\mu\text{M}$ ), as indicated. Scale bars represent 1 nA (vertical) and 50 ms (horizontal) in all cases. (b) Bar graph plotting mean (with S.E.M. bars, from number of cells indicated) % inhibition caused by CORM-2 in the absence or presence of the drugs indicated (taken from studies exemplified by current traces).  $***P < 0.001$  (effects of CORM-2 alone when compared with controls);  $***P < 0.001$  (comparing effects of CORM-2 alone with CORM-2 in the presence of drugs indicated). (c) As in panel (a), except cells were pretreated (1 h at  $37^\circ\text{C}$ ) with DPI (3  $\mu\text{M}$ ), allopurinol (1  $\mu\text{M}$ ), mitoTEMPO (10  $\mu\text{M}$ ) or antimycin A (3  $\mu\text{M}$ ), as indicated, prior to recordings. (d) Bar graph plotting mean (with S.E.M. bars) % inhibition caused by CORM-2 in the absence or presence of the drugs indicated.  $**P < 0.01$ ,  $*P < 0.05$ , comparing the effects of CORM-2 alone or with CORM-2 in the presence of drugs indicated. Dashed line indicates the mean effect of CORM-2 alone. (e) Example currents evoked in hKv1.5-expressing HEK293 cells before and during exposure to 30  $\mu\text{M}$  CORM-2. Currents are examples from time-series studies (as in Figure 1) in which cells were repeatedly depolarized from  $-80$  to  $+50$  mV (100 ms duration, 0.2 Hz). CORM-2 was applied either to untreated cells or to cells pretreated with L-NAME (1 mM; 1 h,  $37^\circ\text{C}$ ), Rp-8-Br-cGMPS (50  $\mu\text{M}$ ; 1 h,  $37^\circ\text{C}$ ) or both agents together, as indicated. Scale bars represent 1 nA (vertical) and 50 ms (horizontal) in all cases; except the L-NAME-treated example (vertical scale bar = 0.2 nA). (f) Bar graph plotting mean (with S.E.M. bars,  $n$  numbers indicated in each bar) % inhibition caused by CORM-2 in the presence of the drugs indicated (taken from studies exemplified by current traces). Mean effect of CORM-2 alone is indicated by the dashed line.  $***P < 0.001$ , significant difference from inhibition caused by CORM-2 alone

complex III of the electron transport chain (Figures 2c and d). Thus mitochondria appear to be the source of ROS involved in CO-mediated inhibition of hKv1.5.

CO is also known to activate NOS and soluble guanylyl cyclase (sGC) in several cell types. Pretreatment of cells (1 h at  $37^\circ\text{C}$ ) with the NOS inhibitor L-NAME (1 mM) significantly attenuated the ability of CORM-2 to inhibit hKv1.5 (Figures 2e and f). Similarly, pretreatment of cells (1 h at  $37^\circ\text{C}$ ) with the membrane-permeable sGC inhibitor, Rp-8-Br-cGMPS (100 nM), significantly reduced the inhibitory effects of CORM-2 on hKv1.5 (Figures 2e and f). Pretreatment of cells with both agents similarly reduced the ability of CO to inhibit currents (Figures 2e and f). These data suggested that CO could stimulate NO formation and this was further confirmed by monitoring NO levels in hKv1.5-expressing HEK293 cells using the NO-sensitive fluoroprobe, DAF-2 (Figures 3a and b). Application of CORM-2 (30  $\mu\text{M}$ ) to DAF-2-loaded cells caused a significant rise in fluorescence, which was fully attenuated following preincubation of cells with 1 mM L-NAME (1 h,  $37^\circ\text{C}$ ). It is likely, therefore, that CO inhibits hKv1.5 in part via activation of NO formation, as a previous study has suggested that NO can inhibit Kv1.5.<sup>30</sup> NO inhibition was shown by Nunez *et al.*<sup>30</sup> to be mediated partly via PKG-dependent phosphorylation, as is the case for CO (Figure 3), and also by

nitrosylation. To explore nitrosylation as a mechanism for CO-mediated inhibition of hKv1.5, we employed the biotin-switch technique and detected nitrosylation of hKv1.5 protein by CORM-2 but not by iCORM (Figure 3c), indicating that CO does indeed stimulate nitrosylation of hKv1.5.

The observation that CO raises ROS levels (presumably levels of superoxide, as SOD mimetics ameliorated the effects of CO; Figure 2), and also raises NO levels suggests the possibility that peroxynitrite ( $\text{ONOO}^-$ ) formation occurs in the presence of CO, as we have previously suggested.<sup>58</sup> In support of this idea, we found that CO increased the level of fluorescence in cells loaded with the  $\text{ONOO}^-$  indicator, 2-[6-(4'-amino)phenoxy-3H-xanthen-3-on-9-yl]benzoic acid (APF; Figure 4a). These rises were fully attenuated by both L-NAME and the  $\text{ONOO}^-$  scavenger, FeTPPS (Figures 4a and b). Furthermore, pretreatment of cells with FeTPPS strongly attenuated the CO-mediated inhibition of hKv1.5 (Figure 4c).

**Exploring the roles of C346 and C331.** Based on structural modelling, it has previously been suggested (but not demonstrated) that two cysteine (C) residues within hKv1.5 might be nitrosylated by NO and thereby account for its inhibitory action on the channel.<sup>28</sup> As much of the effects of CO, as reported here, are mediated by NO formation (Figures 2 and 3), we explored the potential involvement of these two residues, C331 and C346. To do this, we generated C  $\rightarrow$  A (alanine) substitution mutants. As shown in Figure 5, CO was still able to inhibit the activity of the C331A (Figure 5a) and C346A mutant channels (Figure 5b). The degree of inhibition caused by 30  $\mu\text{M}$  CORM-2 ( $44 \pm 8.6\%$ , mean  $\pm$  S.E.M.,  $n=5$ ,  $P < 0.001$  for C331A and  $47 \pm 1.7\%$ ,



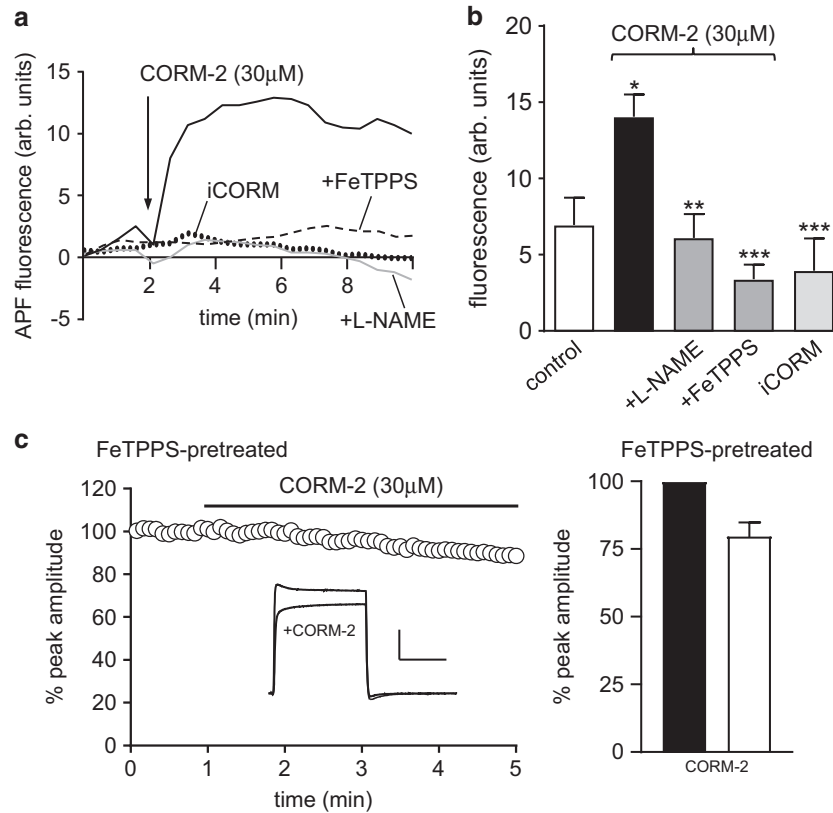


**Figure 4** CO stimulates ONOO formation, which contributes to the inhibition of hKv1.5. (a) Example plots of the fluorescence levels in APF-loaded cells. At the point indicated by the arrow, cells were exposed to 30 μM CORM-2 alone (solid line) or following pretreatment for 1 h at 37 °C with FeTPPS (50 μM; dashed line) or L-NAME (1 mM; grey line). Also shown is the level of fluorescence detected in a cell exposed to 30 μM iCORM (dotted line). (b) Mean level of fluorescence detected in APF-loaded cells 5 min after exposure to CORM-2 alone or in the additional presence of FeTPPS or L-NAME or when exposed to iCORM or no drugs (control). Bars represent mean ± S.E.M. taken from between five and eight cells in each case. (c) Left, time-series plot (generated by repeated step-depolarizations from -80 to +50 mV (100 ms duration, 0.2 Hz)) obtained from a hKv1.5-expressing HEK293 cell previously exposed to 50 μM FeTPPS (1 h at 37 °C). Plot shows normalized peak current amplitudes. For the period indicated by the horizontal bar, the cell was exposed to 30 μM CORM-2. Inset shows example currents before and during CORM-2 exposure (scale bars: 1 nA (vertical), 50 ms (horizontal)). Right, bar graph showing the mean (± S.E.M.; n = 5 cells) effects of CORM-2 following pretreatment with FeTPPS

study indicates that Kv1.5 is uniquely inhibited by CO acting via all of the aforementioned pathways as well as via cGMP formation, which presumably modifies channel activity via phosphorylation as suggested previously for the effects of NO.<sup>30</sup>

Each of these distinct means of Kv1.5 regulation by CO can be regarded as potentially important under varying physiological and pathological conditions, not only in the heart but also in the vasculature. Recent studies have provided evidence that H<sub>2</sub>O<sub>2</sub> generated by cardiac myocytes couples cardiac metabolism to coronary flow by activating Kv1.5 channels in coronary VSMCs, which presumably leads to their relaxation (and hence vessel dilation) due to hyperpolarization and reduced Ca<sup>2+</sup> influx.<sup>33–35</sup> CO raises ROS levels, yet reverses augmentation of Kv1.5 by H<sub>2</sub>O<sub>2</sub> (Figure 6). This would suggest that ROS contributing to Kv1.5 inhibition by CO are likely to be either superoxide derived from mitochondria and/or ONOO<sup>-</sup> formed from superoxide and NO. It is clear that these ROS contribute to channel inhibition, whereas H<sub>2</sub>O<sub>2</sub> has the opposite effect of augmenting current amplitudes – this suggests that Kv1.5 is differentially regulated by different oxidant species. Interestingly, CO-mediated inhibition of hKv1.5 was partly attenuated by the SOD mimetics MnTMPyP

and MnTBAP (Figure 2). These agents would presumably increase H<sub>2</sub>O<sub>2</sub> levels through superoxide dismutation, yet CO reversed the effects of exogenous H<sub>2</sub>O<sub>2</sub> (Figure 6). This finding would suggest that CO-mediated inhibition of Kv1.5 via other mechanisms (e.g., nitrosylation or the sGC/cGMP pathway) can override augmentation by H<sub>2</sub>O<sub>2</sub>. This in turn suggests that CO levels may physiologically regulate H<sub>2</sub>O<sub>2</sub>-mediated coupling of coronary blood flow to cardiac metabolism.

Figures 2 and 3 indicate that NO formation has an important role in Kv1.5 inhibition by CO. Our findings in this regard are consistent with the study of Nunez *et al.*<sup>30</sup> who demonstrated that NO inhibited recombinant hKv1.5 via nitrosylation and a cGMP-dependent mechanism. The present study shows that CO also activates these pathways by stimulating a rise in NO levels. However, NO formation does not account for all of the effects of CO as detailed here. Although molecular modelling suggested C331 and C346 as candidate cysteine residues for nitrosylation,<sup>30</sup> we found that both the C331A and C346A mutants remained sensitive to inhibition by CO (Figure 5). Furthermore, both mutant channels were nitrosylated by CO, suggesting that alternative cysteines in the Kv1.5 channel are preferentially targeted for nitrosylation. Physiologically, this

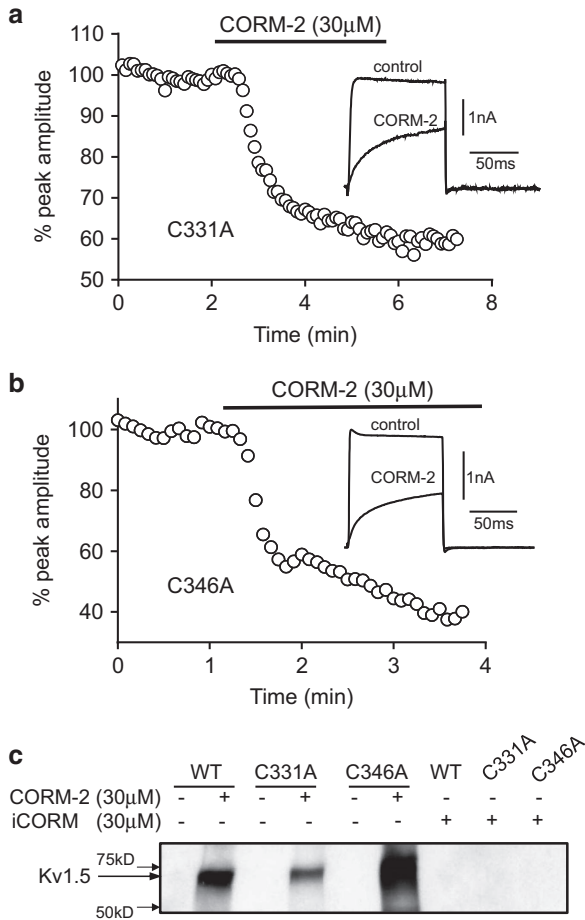


**Figure 5** Mutation of C331 or C346 does not impede CO-mediated inhibition of hKv1.5. (a) Time-series plot (generated by repeated step-depolarizations from  $-80$  to  $+50$  mV (100 ms duration, 0.2 Hz)) obtained from a HEK293 cell stably expressing hKv1.5 containing the C331A mutation. Plot shows normalized peak current amplitudes. For the period indicated by the horizontal bar, the cell was exposed to  $30 \mu\text{M}$  CORM-2. Inset shows example currents recorded before and during CORM-2 application, as indicated. (b) As in panel (a), except currents were recorded from a cell stably expressing hKv1.5 containing the C346A mutation. (c) Nitrosylation of WT and mutant hKv1.5 channels was detected using the biotin-switch assay. Note: nitrosylation of hKv1.5 was only detected in samples treated with CORM-2, not iCORM

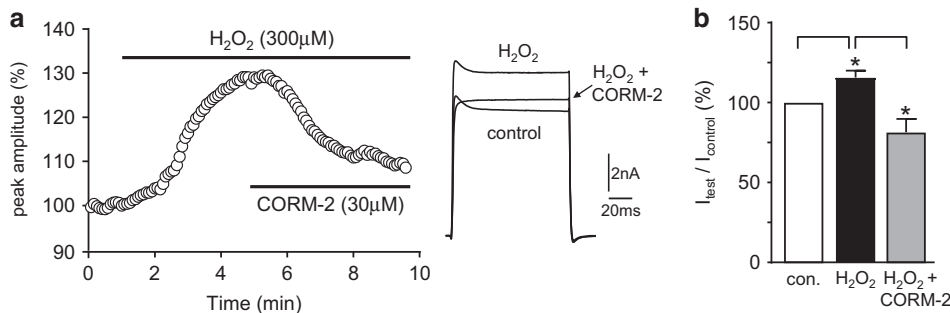


**Figure 6** CO reverses  $\text{H}_2\text{O}_2$ -mediated augmentation of hKv1.5 activity. (a) Left, time-series plot, generated by repeated step-depolarizations from  $-80$  to  $+50$  mV (100 ms duration, 0.2 Hz), obtained from a HEK293 cell stably expressing hKv1.5. Plot shows normalized peak current amplitudes. For the period indicated by the upper horizontal bar, the cell was exposed to  $300 \mu\text{M}$   $\text{H}_2\text{O}_2$ . For the period indicated by the lower bar,  $30 \mu\text{M}$  CORM-2 was also present. Right, example currents evoked before and during  $\text{H}_2\text{O}_2$  application alone or together with CORM-2, as indicated. (b) Bar graph indicating the mean ( $\pm$  S.E.M. ( $n=5$ )) percentage change in current amplitude caused by  $\text{H}_2\text{O}_2$  alone or together with CORM-2, as indicated.  $*P < 0.05$

NO-dependent means by which CO regulates Kv1.5 activity is likely to be important both in the vasculature (particularly but not exclusively the coronary vasculature, as discussed above) and in the heart, where Kv1.5 exerts an important influence in shaping the atrial AP.<sup>20,21</sup> Kv1.5 is an important target for therapies aimed at treating AF,<sup>23,25</sup> and interestingly, maintenance or augmentation of NO bioavailability is also considered a viable approach in the treatment of AF.<sup>41</sup> Our data suggest that increasing CO levels (either via stimulating HO-1 expression or via CO donors<sup>53</sup>) may therefore be of benefit in AF treatment via increased NO formation. However, elevated NO in the presence of superoxide can lead to the formation of ONOO<sup>-</sup> and this was indeed observed in our study (Figure 4). ONOO<sup>-</sup> formation is seen in AF<sup>67,68</sup> and is presumably deleterious. Increased ONOO<sup>-</sup> formation contributes to shortening of the effective refractory period seen in AF, but this is unlikely to arise from inhibition of Kv1.5, as this would be expected to prolong AP duration and therefore, presumably, the effective refractory period.

A noteworthy feature of the CO-mediated inhibition of Kv1.5 was the marked slowing of its activation kinetics (see Figure 1d), which was also prominent in the mutants (Figure 5). Slowing of activation by CO appears strikingly similar to the previously reported slowing of activation caused by zinc.<sup>69</sup> It would appear that this effect cannot be attributed to any particular single pathway of channel inhibition because residual inhibition caused by CO in the presence of SOD mimetics, NO or sGC inhibition or in the presence of FeTPPS to scavenge ONOO<sup>-</sup> was not associated with a slowing of channel activation. This suggests that a combination of these signalling pathways is required in order to observe kinetic changes caused by CO together with channel inhibition.

To explore CO-mediated modulation of Kv1.5 in a more physiological setting, we investigated its ability to regulate K<sup>+</sup> currents in the mouse atrial cell line, HL-1. Our data indicate that CO inhibits a DPO-1-sensitive K<sup>+</sup> current in these cells and so presumably arises at least primarily due to activity of Kv1.5.<sup>60</sup> Our data do not exclude actions of CO on other cardiac ion channels, and indeed a number of such channels are known to be CO sensitive.<sup>61</sup> However, inhibition of Kv1.5 does appear to be of functional significance, as it significantly

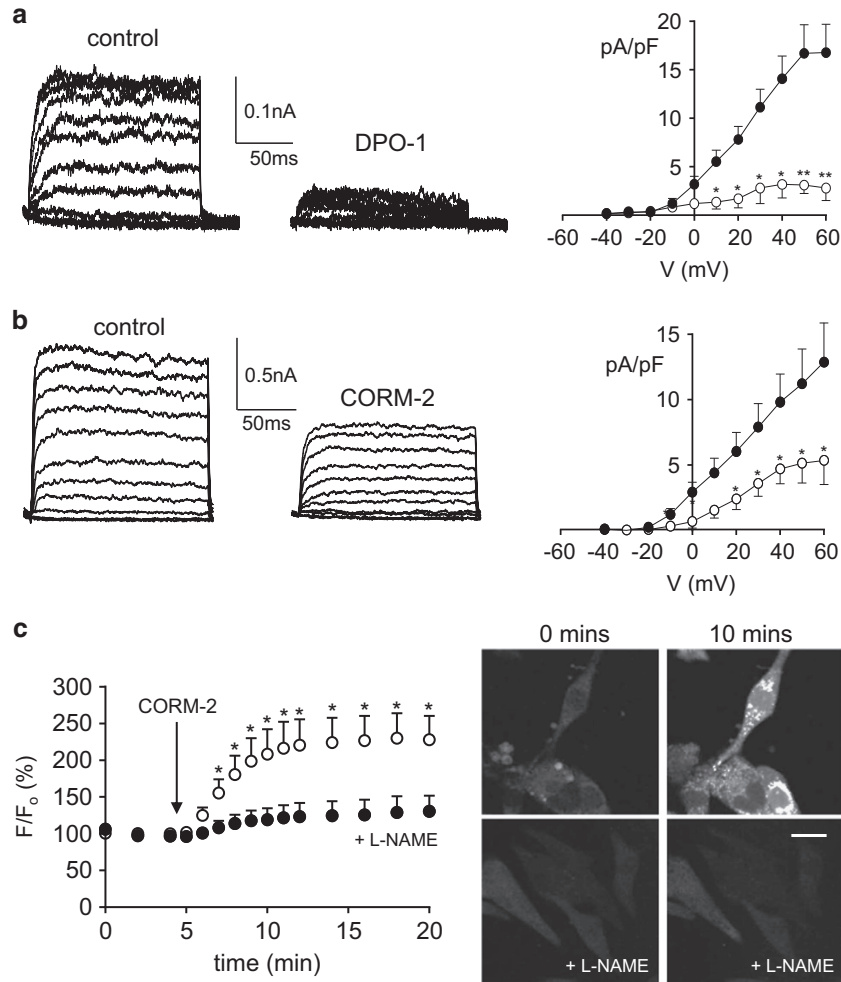


**Figure 7** CO inhibits native K<sup>+</sup> currents and raises NO levels in HL-1 atrial cells. **(a)** Families of outward K<sup>+</sup> currents recorded in an example HL-1 cells by step-depolarizations as described in Methods section, before (control) and during (DPO-1) bath application of the Kv1.5 inhibitor, DPO-1 (1  $\mu$ M). Right, mean ( $\pm$  S.E.M.,  $n=7$  cells) current density versus membrane potential plot before (solid symbols) and during (open symbols) application of 1  $\mu$ M DPO-1. **(b)** Exactly as in panel (a), except cells were exposed to CORM-2 (30  $\mu$ M;  $n=9$ ) rather than DPO-1. **(c)** Left, mean ( $\pm$  S.E.M.) fluorescence recorded in HL-1 cells loaded with the NO indicator, DAF-2. Fluorescence was measured in untreated cells (open circles,  $n=5$ ) or cells pretreated with L-NAME (1 mM; solid circles; 1 h, 37  $^{\circ}$ C;  $n=5$ ). Right, example images at 0 and 10 min after commencement of CORM-2 application, as indicated, in untreated and L-NAME-treated cells. Scale bar (20  $\mu$ m) applies to all images. In all panels, \*\* $P<0.01$ , \* $P<0.05$

increased AP amplitude and duration in a manner that was both mimicked and occluded by DPO-1. Thus CO regulation of Kv1.5 is potentially of physiological significance for regulating atrial excitability. It may also be of pathological significance, for example, in atrial fibrillation, which is associated with increased expression of HO-1.<sup>54,56</sup>

In summary, we have demonstrated that CO inhibits both native (mouse) and recombinant (human) Kv1.5 and does so via multiple signalling pathways. Tonic regulation of Kv1.5 by CO is likely to be of physiological relevance in cardiac atria as well as vascular smooth muscle, where it may regulate channel responses to other signalling factors (e.g., H<sub>2</sub>O<sub>2</sub>). The significance of Kv1.5 regulation by CO may increase under pathological conditions such as atrial fibrillation and vascular disease due to increased HO-1 expression.

**Materials and Methods**

**Generation and culture of HEK293 cells expressing Kv1.5.** Wild-type (WT) human Kv1.5 (KCNA5) cDNA was amplified from a human foetal brain

cDNA library (Clontech, Wooburn Green, Buckinghamshire, UK) using the primers: 5'-TGGAATTCACCATGGAGATCGCCTG-3' and 5'-GACTCGAGTCACAAATCTGTTTCCCG-3' (Sigma-Aldrich, Gillingham, Dorset, UK) in a touchdown PCR. The  $\approx$ 1.7 kb product was cloned using the CloneJET Kit (Thermo Fisher Scientific, Loughborough, Leicestershire, UK) and then subcloned into pcDNA6 (Invitrogen, Loughborough, Leicestershire, UK) using EcoRI and XhoI restriction enzymes (New England Biolabs, Hitchin, Hertfordshire, UK). At each step, clones were confirmed by Sanger sequencing (Genewiz, Bishop's Stortford, Hertfordshire, UK).

HEK293 cells were cultured in MEM with Earle's salts and L-glutamine, supplemented with 9% (v/v) fetal calf serum (GloboPharm, Esher, Surrey, UK), 1% (v/v) non-essential amino acids, 50  $\mu$ g/ml gentamicin, 100 units/ml penicillin G, 100  $\mu$ g/ml streptomycin and 0.25  $\mu$ g/ml amphotericin in a humidified atmosphere of air/CO<sub>2</sub> (19 : 1) at 37  $^{\circ}$ C. All cell culture reagents were purchased from Gibco-BRL (ThermoFisher Scientific) unless otherwise stated. To generate stable HEK293/Kv1.5 cell lines, cells were transfected with either a pcDNA6/Kv1.5(WT) or pcDNA6/Kv1.5 (Mutant) construct using the PolyFect transfection reagent (Qiagen, Hybaid Ltd, Teddington, UK) according to the manufacturer's instructions. Stable HEK293/Kv1.5 cell lines were achieved by antibiotic selection with blasticidin (5  $\mu$ g/ml, ThermoFisher Scientific), added to the medium 3 days after transfection. Selection was applied for 4 weeks (media changed every 4–5 days), after which time individual colonies were picked and seeded in T25 flasks and allowed to reach confluence. They were then

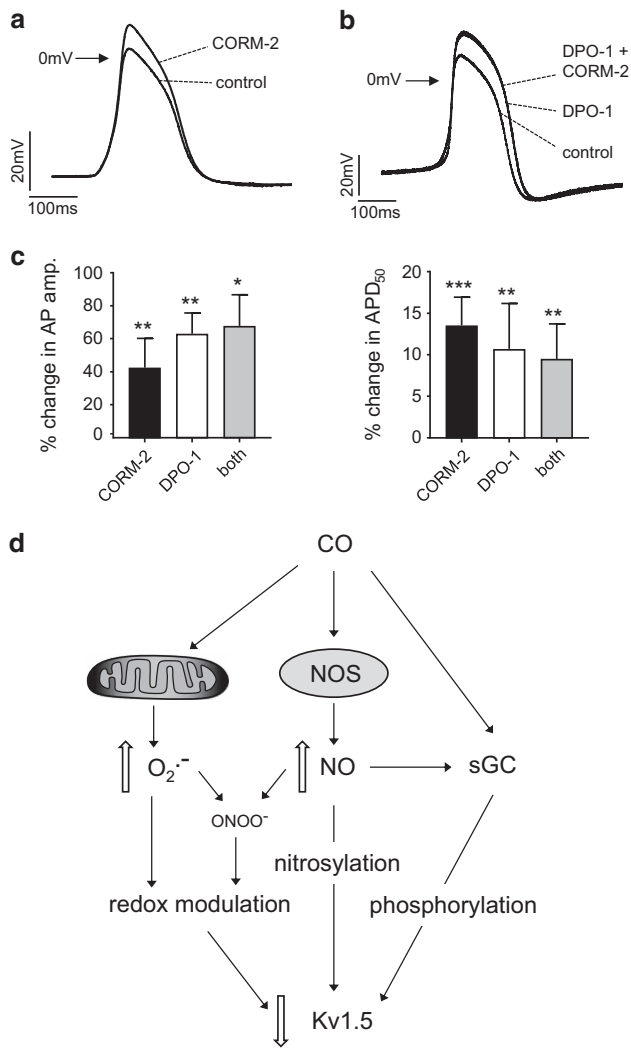


**Figure 8** CO augments action potentials in HL-1 cells. **(a)** Spontaneous action potentials (APs) recorded in an example HL-1 cell before (control) and during application of 30  $\mu\text{M}$  CORM-2. Note: CORM-2 increases the AP amplitude and duration. **(b)** As in panel (a), except that the cell was exposed to DPO-1 (1  $\mu\text{M}$ ), then CORM-2 (30  $\mu\text{M}$ ) in the continued presence of DPO-1. Note: DPO-1 augments APs and prevents further augmentation by CORM-2. **(c)** Mean ( $\pm$  S.E.M.) augmentation in AP amplitude (AP amp.; left) and APD<sub>50</sub> (right) caused by CORM-2 alone ( $n=10$ ), DPO-1 ( $n=9$ ) alone or CORM-2 in the continued presence of DPO-1 (both;  $n=8$ ). Significant difference from control (no drug): \*\*\* $P<0.001$ , \*\* $P<0.01$ , \* $P<0.05$ . There were no significant differences between the conditions. **(d)** Schematic mechanism for the inhibition of Kv1.5 by CO. Data presented suggest CO increases ROS (presumably superoxide, O<sub>2</sub><sup>-</sup>) formation from mitochondria, which may directly regulate Kv1.5, but can also combine with NO (levels of which increase in response to CO) to form peroxynitrite (ONOO<sup>-</sup>) to cause channel inhibition. Elevated NO levels also directly nitrosylate Kv1.5. CO can also stimulate sGC (an effect that is also promoted by elevated NO levels), which leads to channel phosphorylation

transferred to T75 flasks for further culture and examination of K<sup>+</sup> currents. Cells were harvested from culture flasks by trypsinization and plated onto coverslips 24–48 h before use in electrophysiological studies. Blastocidin selection was maintained throughout the entire cloning process at 5  $\mu\text{g}/\text{ml}$  and then subsequently reduced to 2.5  $\mu\text{g}/\text{ml}$  in all subsequent passages of cells once stable clones had been positively identified.

The C331A and C346A mutations were introduced into WT human Kv1.5 (hKv1.5, in pcDNA6) using the Quik-Change Site-Directed Mutagenesis Kit (Stratagene,

Cheadle, UK) according to the manufacturer's instructions. All constructs were verified by DNA sequence analysis before transfection.

**Culture of HL-1 cells.** HL-1 atrial cardiomyocytes were maintained in Claycomb media (Sigma, UK) supplemented with batch-specific 10% FBS (Sigma, Gillingham), 1% penicillin/streptomycin (Invitrogen), 0.1 mM norepinephrine (Sigma) and 2 mM l-glutamine (Invitrogen). Cells were cultured in flasks, or on coverslips, pretreated with 0.02% Bacto gelatin (Fisher Scientific, Loughborough, UK) and 0.5% fibronectin (Invitrogen).

**Exposure to CO.** CO was applied to HEK293 cells and HL-1 cells via the CORM, CORM-2. CORM-2 was prepared no longer than 1 h before use by dissolving in dimethylsulphoxide (DMSO) at a stock concentration of 30 mM so that dilution into perfusate or other solutions in which cells were maintained (e.g., electrophysiology, imaging, biotin switch assay) usually resulted in DMSO levels of no more than 1 : 1000. iCORM, which served as a negative control, was prepared by dissolving CORM-2 identically and leaving in perfusate solution for 2 weeks prior to use, by which time all CO was released and lost from solution.

**Electrophysiology.** Coverslips with cultured cells were transferred from the incubator into a recording chamber mounted on the stage of an Olympus CK40 inverted microscope (Olympus, London, UK) and continually perfused with bath solution (2–4 ml.min<sup>-1</sup>) containing the following: 140 mM NaCl, 4 mM KCl, 2 mM CaCl<sub>2</sub>, 1 mM MgCl<sub>2</sub>, 5 mM glucose, buffered with 10 mM HEPES, pH 7.4. Single cells were selected for whole-cell patch-clamp experiments at 22  $\pm$  1 °C. Pipettes were filled with intracellular solution (140 mM KCl, 10 mM NaCl, 4 mM MgCl<sub>2</sub>, 20 mM EGTA, 10 mM HEPES, pH 7.2) and had a resistance of 4–6 M $\Omega$ . Whole-cell voltage-clamp or current-clamp experiments were recorded, digitized and stored with an Axopatch 200B amplifier, Digidata 1322A and pCLAMP 10 respectively (Molecular Devices, Union City, CA, USA).

Series resistance was compensated by 70–90%. If a significant increase in series resistance occurred (>20%), the experiment was terminated. Leak currents were subtracted using the P/4 protocol in the pCLAMP software and voltage-clamp signals were sampled at 50 kHz and low-pass filtered at 20 kHz; *I*-*V* relationships were measured by stepping from a holding potential of -90 mV to voltages between -60 and +80 mV in 10 mV increments for 500 ms. Time-series experiments were measured using a single pulse protocol stepping from -90 to +50 mV for 100 ms every 5 s.

HL-1 spontaneous APs were acquired in gap-free mode with no current injected. I<sub>K<sub>ur</sub> was recorded as described previously<sup>70</sup> using a 100 ms prepulse to +40 mV to inactivate I<sub>to1</sub>, followed by a 150 ms test pulse from -50 to between -40 and +50, then to -30 mV.</sub>

Offline analysis was performed using the data analysis package Clampfit 10.0 (Molecular Devices, Foster City, CA, USA), and subsequent fitting and statistical analysis was undertaken using GraphPad Prism 7 (GraphPad Software, La Jolla, CA, USA). Results are presented as means  $\pm$  S.E.M., with 'n' representing the number of experiments performed. Statistical significance was evaluated using unpaired Student's *t*-tests where differences were considered significant when the *P*-value was < 0.05.

**Biotin-switch assay.** Detection of S-nitrosylated hKv1.5 was performed using the biotin-switch assay followed by western blotting as previously described.<sup>71</sup> Briefly, HEK293 cells expressing WT or mutant (C331A or C346A) Kv1.5 were harvested and lysed in a non-denaturing solution (in mM: 50 Tris-HCl, 300 NaCl, 5 EDTA, and 1% Triton-X). Extracts were adjusted to 0.5 mg/ml and incubated with CORM-2 (30  $\mu\text{M}$ ) for 15 min at 37 °C; inactive CORM (iCORM, 30  $\mu\text{M}$ ) and DMSO were used as controls.

CORM-2 and iCORM were removed and buffered exchanged using desalting spin columns (Thermo Fisher Scientific). From this point, all procedures were carried out in the dark. Lysates were incubated in blocking buffer (in mM: 225 HEPES, 0.9 EDTA, 20 methyl methanethiosulfonate (MMTS), and 2.5% SDS, pH 7.4) for 20 min at 50 °C with agitation. Lysates were subjected to buffer exchange to remove MMTS and eluted in HENS buffer (mM: 250 HEPES, 1 EDTA, and 1% SDS, pH 7.4) and incubated with 1/3 volume of *N*-[6-(biotinamido)hexyl]-3'-(2'-pyridylidithio) propionamide (biotin-HPDP, Pierce, Loughborough, UK) and ascorbate (1 mM) for 1 h at room temperature, followed by buffer exchange to remove biotin-HPDP from the samples. Unless otherwise stated, all buffers were supplemented with protease inhibitor cocktail tablets (Roche, Welwyn Garden City, UK).



Biotinylated proteins were detected via western blotting as described previously.<sup>28</sup> Protein samples were prepared without reducing agents and were not boiled before electrophoresis to prevent the reversal of cysteine biotinylation and non-specific biotin–HPDP reactions, respectively.

**Fluorescence detection of nitric oxide (NO) and peroxynitrite (ONOO<sup>-</sup>).** Cells were plated on coverslips and allowed to grow for 48 h at 37 °C in a humidified atmosphere containing 95% air and 5% CO<sub>2</sub> before being preincubated for 1 h with DAF-2 diacetate (5 μM; Invitrogen), prepared in the following extracellular solution: 140 mM NaCl, 4 mM KCl, 1.5 mM CaCl<sub>2</sub>, 2 mM MgCl<sub>2</sub>, 10 mM HEPES, 10 mM glucose, pH 7.4). Cells were then gently washed twice with extracellular solution and then left for at least 15 min in an incubator to allow the hydrolysis of DAF-2 diacetate into the free NO-sensitive free acid form (DAF-2).

Fragments of coverslip with attached cells were placed on a Zeiss (Oberkochen, Germany) laser scanning confocal microscope (LSM 510) fitted with a ×40 oil immersion lens (Zeiss Plan Neofluar, refractive index of 1.3) and continuously perfused with extracellular solution at a rate of 0.5 ml/min. DAF-2 loaded cells were excited with the 488-nm line of a 20-mW diode laser (attenuated by ~90%), and emitted fluorescence was measured at > 515 nm. *x–y* images were obtained from isolated cells at 1 min intervals to minimize photobleaching using the Zeiss AIM software. Experimental settings were identical in all test conditions and each experiment was repeated five times. Fluorescence intensity of isolated cells was analysed using the ImageJ software (Laboratory for Optical and Computational Instrumentation, Madison, WI, USA) and data are presented as means ± S.E.M.

To detect ONOO<sup>-</sup>, cells grown on coverslips were incubated for 1 h at 37 °C with APF (10 μM) dissolved in HEPES-buffered saline. For L-NAME or FeTPPS experiments, cells were preincubated with either drug at the same time as the APF treatment. Coverslips fragments with cells attached were placed in a chamber (as a static bath set-up) filled with 200 μl of HEPES-buffered saline containing 10 μM APF. Changes in fluorescence intensity were measured over 10 min using a ZEISS (Oberkochen) laser-scanning confocal microscope (LSM 510). APF was excited at 488 nm and emission monitored at 510 nm, and images were obtained using the Zeiss AIM software. All settings were identical for control and test conditions.

## Conflict of Interest

The authors declare no conflict of interest.

**Acknowledgements.** This work was supported by the British Heart Foundation.

## Publisher's Note

Springer Nature remains neutral with regard to jurisdictional claims in published maps and institutional affiliations.

- Ravens U, Wettwer E. Ultra-rapid delayed rectifier channels: molecular basis and therapeutic implications. *Cardiovasc Res* 2011; **89**: 776–785.
- Chung YH, Shin C, Kim MJ, Lee BK, Cha CI. Immunohistochemical study on the distribution of six members of the Kv1 channel subunits in the rat cerebellum. *Brain Res* 2001; **895**: 173–177.
- Jou I, Pyo H, Chung S, Jung SY, Gwag BJ, Joe EH. Expression of Kv1.5 K<sup>+</sup> channels in activated microglia in vivo. *Glia* 1998; **24**: 408–414.
- Comes N, Bielanska J, Vallejo-Gracia A, Serrano-Albarras A, Marruecos L, Gomez D et al. The voltage-dependent K<sup>+</sup> channels Kv1.3 and Kv1.5 in human cancer. *Front Physiol* 2013; **4**: 283.
- Du JY, Yuan F, Zhao LY, Zhu J, Huang YY, Zhang GS et al. Suppression of Kv1.5 protects against endothelial apoptosis induced by palmitate and in type 2 diabetes mice. *Life Sci* 2017; **168**: 28–37.
- Zhang S, Liu B, Fan Z, Wang D, Liu Y, Li J et al. Targeted inhibition of survivin with YM155 promotes apoptosis of hypoxic human pulmonary arterial smooth muscle cells via the upregulation of voltage-dependent K<sup>+</sup> channels. *Mol Med Rep* 2016; **13**: 3415–3422.
- Michelakis ED, Thebaud B, Weir EK, Archer SL. Hypoxic pulmonary vasoconstriction: redox regulation of O<sub>2</sub>-sensitive K<sup>+</sup> channels by a mitochondrial O<sub>2</sub>-sensor in resistance artery smooth muscle cells. *J Mol Cell Cardiol* 2004; **37**: 1119–1136.
- Archer SL, Reeve HL, Michelakis E, Puttagunta L, Waite R, Nelson DP et al. O<sub>2</sub> sensing is preserved in mice lacking the gp91 phox subunit of NADPH oxidase. *Proc Natl Acad Sci USA* 1999; **96**: 7944–7949.
- Archer SL, Gomberg-Maitland M, Maitland ML, Rich S, Garcia JG, Weir EK. Mitochondrial metabolism, redox signaling, and fusion: a mitochondria-ROS-HIF-1α-Kv1.5 O<sub>2</sub>-sensing pathway at the intersection of pulmonary hypertension and cancer. *Am J Physiol Heart Circ Physiol* 2008; **294**: H570–H578.
- Platoshyn O, Golovina VA, Bailey CL, Limswan A, Krick S, Juhaszova M et al. Sustained membrane depolarization and pulmonary artery smooth muscle cell proliferation. *Am J Physiol Cell Physiol* 2000; **279**: C1540–C1549.
- Burg ED, Remillard CV, Yuan JX. Potassium channels in the regulation of pulmonary artery smooth muscle cell proliferation and apoptosis: pharmacotherapeutic implications. *Br J Pharmacol* 2008; **153**(Suppl 1): S99–S111.
- Weir EK, Lopez-Barneo J, Buckler KJ, Archer SL. Acute oxygen-sensing mechanisms. *N Engl J Med* 2005; **353**: 2042–2055.
- Yuan XJ, Wang J, Juhaszova M, Gaine SP, Rubin LJ. Attenuated K<sup>+</sup> channel gene transcription in primary pulmonary hypertension. *Lancet* 1998; **351**: 726–727.
- Remillard CV, Tigno DD, Platoshyn O, Burg ED, Brevnova EE, Conger D et al. Function of Kv1.5 channels and genetic variations of KCNA5 in patients with idiopathic pulmonary arterial hypertension. *Am J Physiol Cell Physiol* 2007; **292**: C1837–C1853.
- Baliga RS, MacAllister RJ, Hobbs AJ. New perspectives for the treatment of pulmonary hypertension. *Br J Pharmacol* 2011; **163**: 125–140.
- Ko EA, Han J, Jung ID, Park WS. Physiological roles of K<sup>+</sup> channels in vascular smooth muscle cells. *J Smooth Muscle Res* 2008; **44**: 65–81.
- Cox RH. Molecular determinants of voltage-gated potassium currents in vascular smooth muscle. *Cell Biochem Biophys* 2005; **42**: 167–195.
- Chen TT, Luykenaar KD, Walsh EJ, Walsh MP, Cole WC. Key role of Kv1 channels in vasoregulation. *Circ Res* 2006; **99**: 53–60.
- Ohanyan V, Yin L, Bardakjian R, Kolz C, Enrick M, Hakobyan T et al. Requisite role of Kv1.5 channels in coronary metabolic dilation. *Circ Res* 2015; **117**: 612–621.
- Wettwer E, Hala O, Christ T, Heubach JF, Dobrev D, Knaut M et al. Role of IKur in controlling action potential shape and contractility in the human atrium: influence of chronic atrial fibrillation. *Circulation* 2004; **110**: 2299–2306.
- Schmitt N, Grunnet M, Olesen SP. Cardiac potassium channel subtypes: new roles in repolarization and arrhythmia. *Physiol Rev* 2014; **94**: 609–653.
- Ford J, Milnes J, El HS, Wettwer E, Loose S, Matschke K et al. The positive frequency-dependent electrophysiological effects of the IKur inhibitor XEN-D0103 are desirable for the treatment of atrial fibrillation. *Heart Rhythm* 2016; **13**: 555–564.
- Ravens U, Odening KE. Atrial fibrillation: therapeutic potential of atrial K<sup>+</sup> channel blockers. *Pharmacol Ther* 2016; **176**: 13–21.
- Heijman J, Algalarrondo V, Voigt N, Melka J, Wehrens XH, Dobrev D et al. The value of basic research insights into atrial fibrillation mechanisms as a guide to therapeutic innovation: a critical analysis. *Cardiovasc Res* 2016; **109**: 467–479.
- Grandi E, Maleckar MM. Anti-arrhythmic strategies for atrial fibrillation: the role of computational modeling in discovery, development, and optimization. *Pharmacol Ther* 2016; **168**: 126–142.
- Benson MD, Li QJ, Kieckhafer K, Dudek D, Whorton MR, Sunahara RK et al. SUMO modification regulates inactivation of the voltage-gated potassium channel Kv1.5. *Proc Natl Acad Sci USA* 2007; **104**: 1805–1810.
- Jindal HK, Folco EJ, Liu GX, Koren G. Posttranslational modification of voltage-dependent potassium channel Kv1.5: COOH-terminal palmitoylation modulates its biological properties. *Am J Physiol Heart Circ Physiol* 2008; **294**: H2012–H2021.
- Mason HS, Latten MJ, Godoy LD, Horowitz B, Kenyon JL. Modulation of Kv1.5 currents by protein kinase A, tyrosine kinase, and protein tyrosine phosphatase requires an intact cytoskeleton. *Mol Pharmacol* 2002; **61**: 285–293.
- Williams CP, Hu N, Shen W, Mashburn AB, Murray KT. Modulation of the human Kv1.5 channel by protein kinase C activation: role of the Kvβ2.1 subunit. *J Pharmacol Exp Ther* 2002; **302**: 545–550.
- Nunez L, Vaquero M, Gomez R, Caballero R, Mateos-Caceres P, Macaya C et al. Nitric oxide blocks hKv1.5 channels by S-nitrosylation and by a cyclic GMP-dependent mechanism. *Cardiovasc Res* 2006; **72**: 80–89.
- Archer SL, Souil E, Dinh-Xuan AT, Schremmer B, Mercier JC, El YA et al. Molecular identification of the role of voltage-gated K<sup>+</sup> channels, Kv1.5 and Kv2.1, in hypoxic pulmonary vasoconstriction and control of resting membrane potential in rat pulmonary artery myocytes. *J Clin Invest* 1998; **101**: 2319–2330.
- Olschewski A, Weir EK. Redox regulation of ion channels in the pulmonary circulation. *Antioxid Redox Signal* 2015; **22**: 465–485.
- Saitoh S, Kiyooka T, Rocic P, Rogers PA, Zhang C, Swafford A et al. Redox-dependent coronary metabolic dilation. *Am J Physiol Heart Circ Physiol* 2007; **293**: H3720–H3725.
- Saitoh S, Zhang C, Tune JD, Potter B, Kiyooka T, Rogers PA et al. Hydrogen peroxide: a feed-forward dilator that couples myocardial metabolism to coronary blood flow. *Arterioscler Thromb Vasc Biol* 2006; **26**: 2614–2621.
- Rogers PA, Dick GM, Knudson JD, Focardi M, Bratz IN, Swafford AN Jr et al. H<sub>2</sub>O<sub>2</sub>-induced redox-sensitive coronary vasodilation is mediated by 4-aminopyridine-sensitive K<sup>+</sup> channels. *Am J Physiol Heart Circ Physiol* 2006; **291**: H2473–H2482.
- Caouette D, Dongmo C, Berube J, Fournier D, Daleau P. Hydrogen peroxide modulates the Kv1.5 channel expressed in a mammalian cell line. *Naunyn Schmiedebergs Arch Pharmacol* 2003; **368**: 479–486.
- Schulz R, Rassaf T, Massion PB, Kelm M, Balligand JL. Recent advances in the understanding of the role of nitric oxide in cardiovascular homeostasis. *Pharmacol Ther* 2005; **108**: 225–256.

38. Simon JN, Ziberna K, Casadei B. Compromised redox homeostasis, altered nitroso-redox balance and therapeutic possibilities in atrial fibrillation. *Cardiovasc Res* 2016; **109**: 510–518.
39. Kraehling JR, Sessa WC. Contemporary approaches to modulating the nitric oxide-cGMP pathway in cardiovascular disease. *Circ Res* 2017; **120**: 1174–1182.
40. Youn JY, Zhang J, Zhang Y, Chen H, Liu D, Ping P *et al*. Oxidative stress in atrial fibrillation: an emerging role of NADPH oxidase. *J Mol Cell Cardiol* 2013; **62**: 72–79.
41. Carnicer R, Crabtree MJ, Sivakumaran V, Casadei B, Kass DA. Nitric oxide synthases in heart failure. *Antioxid Redox Signal* 2013; **18**: 1078–1099.
42. Polhemus DJ, Lefer DJ. Emergence of hydrogen sulfide as an endogenous gaseous signaling molecule in cardiovascular disease. *Circ Res* 2014; **114**: 730–737.
43. Andreadou I, Iliodromitis EK, Rassaf T, Schulz R, Papapetropoulos A, Ferdinandy P. The role of gasotransmitters NO, H<sub>2</sub>S and CO in myocardial ischaemia/reperfusion injury and cardioprotection by preconditioning, postconditioning and remote conditioning. *Br J Pharmacol* 2015; **172**: 1587–1606.
44. Graser T, Vedernikov YP, Li DS. Study on the mechanism of carbon monoxide induced endothelium-independent relaxation in porcine coronary artery and vein. *Biomed Biochim Acta* 1990; **49**: 293–296.
45. Johnson RA, Teran FJ, Durante W, Peyton KJ, Johnson FK. Enhanced heme oxygenase-mediated coronary vasodilation in Dahl salt-sensitive hypertension. *Am J Hypertens* 2004; **17**: 25–30.
46. Leffler CW, Partenova H, Jaggar JH, Wang R. Carbon monoxide and hydrogen sulfide: gaseous messengers in cerebrovascular circulation. *J Appl Physiol* 2006; **100**: 1065–1076.
47. Rytter SW, Alam J, Choi AM. Heme oxygenase-1/carbon monoxide: from basic science to therapeutic applications. *Physiol Rev* 2006; **86**: 583–650.
48. Chang T, Wu L, Wang R. Inhibition of vascular smooth muscle cell proliferation by chronic hemin treatment. *Am J Physiol Heart Circ Physiol* 2008; **295**: H999–H1007.
49. Otterbein LE, Zuckerman BS, Haga M, Liu F, Song R, Usheva A *et al*. Carbon monoxide suppresses arteriosclerotic lesions associated with chronic graft rejection and with balloon injury. *Nat Med* 2003; **9**: 183–190.
50. Durante W, Johnson FK, Johnson RA. Role of carbon monoxide in cardiovascular function. *J Cell Mol Med* 2006; **10**: 672–686.
51. Durante W. Heme oxygenase-1 in growth control and its clinical application to vascular disease. *J Cell Physiol* 2003; **195**: 373–382.
52. Foresti R, Bani-Hani MG, Motterlini R. Use of carbon monoxide as a therapeutic agent: promises and challenges. *Intensive Care Med* 2008; **34**: 649–658.
53. Motterlini R, Otterbein LE. The therapeutic potential of carbon monoxide. *Nat Rev Drug Discov* 2010; **9**: 728–743.
54. Corradi D, Callegari S, Maestri R, Benussi S, Bosio S, De PG *et al*. Heme oxygenase-1 expression in the left atrial myocardium of patients with chronic atrial fibrillation related to mitral valve disease: its regional relationship with structural remodeling. *Hum Pathol* 2008; **39**: 1162–1171.
55. Yeh YH, Kuo CT, Chang GJ, Chen YH, Lai YJ, Cheng ML *et al*. Rosuvastatin suppresses atrial tachycardia-induced cellular remodeling via Akt/Nrf2/heme oxygenase-1 pathway. *J Mol Cell Cardiol* 2015; **82**: 84–92.
56. Yeh YH, Hsu LA, Chen YH, Kuo CT, Chang GJ, Chen WJ. Protective role of heme oxygenase-1 in atrial remodeling. *Basic Res Cardiol* 2016; **111**: 58.
57. Peers C, Boyle JP, Scragg JL, Dallas ML, Al-Owais MM, Hettiarachchi NT *et al*. Diverse mechanisms underlying the regulation of ion channels by carbon monoxide. *Br J Pharmacol* 2015; **172**: 1546–1556.
58. Hettiarachchi NT, Boyle JP, Bauer CC, Dallas ML, Pearson HA, Hara S *et al*. Peroxynitrite mediates disruption of Ca(2+) homeostasis by carbon monoxide via Ca(2+) ATPase degradation. *Antioxid Redox Signal* 2012; **17**: 744–755.
59. Claycomb WC, Lanson NA Jr., Stallworth BS, Egeland DB, Delcarpio JB, Bahinski A *et al*. HL-1 cells: a cardiac muscle cell line that contracts and retains phenotypic characteristics of the adult cardiomyocyte. *Proc Natl Acad Sci USA* 1998; **95**: 2979–2984.
60. Lagrutta A, Wang J, Fermi B, Novel Salata JJ. potent inhibitors of human Kv1.5K<sup>+</sup> channels and ultrarapidly activating delayed rectifier potassium current. *J Pharmacol Exp Ther* 2006; **317**: 1054–1063.
61. Peers C, Steele DS. Carbon monoxide: a vital signalling molecule and potent toxin in the myocardium. *J Mol Cell Cardiol* 2012; **52**: 359–365.
62. Peers C. Ion channels as target effectors for carbon monoxide. *Exp Physiol* 2011; **96**: 836–839.
63. Dallas ML, Yang Z, Boyle JP, Boycott HE, Scragg JL, Milligan CJ *et al*. Carbon monoxide induces cardiac arrhythmia via induction of the late Na<sup>+</sup> current. *Am J Respir Crit Care Med* 2012; **186**: 648–656.
64. Elies J, Dallas ML, Boyle JP, Scragg JL, Duke A, Steele DS *et al*. Inhibition of the cardiac Na<sup>+</sup> channel Nav1.5 by carbon monoxide. *J Biol Chem* 2014; **289**: 16421–16429.
65. Scragg JL, Dallas ML, Wilkinson JA, Varadi G, Peers C. Carbon monoxide inhibits L-type Ca<sup>2+</sup> channels via redox modulation of key cysteine residues by mitochondrial reactive oxygen species. *J Biol Chem* 2008; **283**: 24412–24419.
66. Al-Owais MM, Hettiarachchi NT, Kirton HM, Hardy ME, Boyle JP, Scragg JL *et al*. A key role for peroxynitrite-mediated inhibition of cardiac ether-a-go-go-related gene (Kv11.1) K<sup>+</sup> channels in carbon monoxide-induced proarrhythmic early afterdepolarizations. *FASEB J* 2017; (doi:10.1096/fj.201700259R).
67. Carnes CA, Chung MK, Nakayama T, Nakayama H, Baliga RS, Piao S *et al*. Ascorbate attenuates atrial pacing-induced peroxynitrite formation and electrical remodeling and decreases the incidence of postoperative atrial fibrillation. *Circ Res* 2001; **89**: E32–E38.
68. Lenaerts I, Driesen RB, Hermida N, Holemans P, Heidbuchel H, Janssens S *et al*. Role of nitric oxide and oxidative stress in a sheep model of persistent atrial fibrillation. *Europace* 2013; **15**: 754–760.
69. Zhang S, Kwan DC, Fedida D, Kehl SJ. External K<sup>+</sup> relieves the block but not the gating shift caused by Zn(2+) in human Kv1.5 potassium channels. *J Physiol* 2001; **532**: 349–358.
70. Gao Z, Lau CP, Chiu SW, Li GR. Inhibition of ultra-rapid delayed rectifier K<sup>+</sup> current by verapamil in human atrial myocytes. *J Mol Cell Cardiol* 2004; **36**: 257–263.
71. Forrester MT, Foster MW, Benhar M, Stamler JS. Detection of protein S-nitrosylation with the biotin-switch technique. *Free Radic Biol Med* 2009; **46**: 119–126.



**Cell Death and Disease** is an open-access journal published by **Nature Publishing Group**. This work is licensed under a **Creative Commons Attribution 4.0 International License**. The images or other third party material in this article are included in the article's Creative Commons license, unless indicated otherwise in the credit line; if the material is not included under the Creative Commons license, users will need to obtain permission from the license holder to reproduce the material. To view a copy of this license, visit <http://creativecommons.org/licenses/by/4.0/>

© The Author(s) 2017